



Biosynthesis of ZnO nanoparticles by heavy metal resistant bacteria

Shilpa Hosmani, Gayathri Devaraja*

Department of Studies in Microbiology, Davangere University, Shivagangothri, Davangere, Karnataka, India

Corresponding Author: Gayathri Devaraja

Abstract

The production of ZnO nanoparticles has attracted significant attention due to their antibacterial and eco-friendly properties. It has also garnered significant interest due to their broad antibacterial and eco-friendly activity. This study focuses on the biosynthesis of ZnONPs using isolated bacterial strains. Molecular identification revealed a high similarity with organisms through 16S ribosomal RNA sequencing. The appearance of white precipitate at the end of the incubation period confirmed the production of ZnONPs. Characterization of Zn nanoparticles was performed using X-ray Diffraction (XRD), Fourier transform infrared spectroscopy (FTIR), Energy Dispersive X-ray Spectroscopy (EDX) and Scanning Electron Microscopy (SEM).

Keywords: Biosynthesis, XRD, FTIR, EDX, SEM, ZnO NPs

Introduction

In recent decades, there has been significant focus on synthesizing a variety of metal and metal oxide nanoparticles with different sizes and morphologies. Currently, the research on nano-sized materials is intense, due to their superior chemical and physical properties compared to bulk structured materials of the same composition. As the field of nanotechnology rapidly advances, the applications of nanosized materials have broadened significantly, ranging from biomedical uses to various industrial applications. Zinc Oxide (ZnO) nanostructures are renowned for their numerous potential applications due to their unique optical, electrical and mechanical characteristics (Mahdi *et al.*, 2020). Zinc oxide finds use in UV filtration, solar cells, photocatalysis, light emitting diodes, memory devices, piezoelectric transducers, photodetectors. Additionally, it is utilized in the creation of electrochemical sensors and biosensors. ZnO's other applications span wastewater treatment, textiles, sunscreens, composites, the food industry, dental cements and drug delivery system especially cancer treatment. It also serves as an anti-bacterial and anti-fungal agent. Zinc oxide nanoparticles (ZnO NPs) can be synthesized via various chemical and physical methods, including sol-gel, hydrothermal, solvothermal, spray pyrolysis, chemical vapor deposition, laser exposure. These methods have been employed for producing nanoparticles with diverse shapes, sizes and highly specific surface structures. Nevertheless, many of these synthesis techniques are toxic chemicals, which are harmful to the environment and human health, thus limiting their application particularly in the medical, pharmaceutical and cosmetics sectors. Consequently, researchers aim to develop green synthesis method to produce nanoparticles with high-yield and desired properties in an environmentally friendly way.

Nanotechnology entails the intentional manipulation of matter on a nanoscale, focusing on the design and characterization of structures, devices and system (Cheng-Hsien, 2007) [2]. A critical component of nanotechnology is the creation of sustainable and ecofriendly technologies for producing nanoparticles with diverse sizes, shapes, chemical compositions and controlled dispersity. Metallic

nanoparticles and metal oxide nanoparticles have broad biomedical applications, attributed to their large surface area to volume ratio and increased reactivity compared to bulk materials. These nanoparticles can be synthesized using chemical and biological methods (Elsa *et al.*, 2016). Green synthesis routes, which avoid the generation of hazardous by products, offer cost effective, non-toxic and environmentally friendly alternatives. Various microorganisms including fungi, bacteria, yeast, algae and viruses have been harnessed for nanoparticle synthesis due to their roles in the bioremediation of toxic metals through metal ion reduction, effectively functioning as nanofactories. The advantages of these biological methods include the ability to scale up processes, economic feasibility, and ease of biomass handling, resulting in high quality nanoparticles with good monodispersity and well-defined dimensions (Zhang *et al.*, 2011) [3]. Zinc oxide nanoparticles have a wide variety of application in medicine, where they are used as chemotherapeutic agents (Wang *et al.*, 2009; Hanley *et al.*, 2008) [4, 5]. It is also used as drug carrier and in the treatment of leukemia and carcinoma cancer cells.

Apart from this, zinc oxide nanoparticle can be used as photocatalyst in photodegradation of environmental organic and toxic pollutants (Yumak *et al.*, 2011). The advantage of using zinc oxide as antimicrobial agent is that they contain mineral elements essential for human and exhibit strong activity even administered in small amount (Jayaseelan *et al.*, 2012) [7]. The present study was focused on the biosynthesis of zinc oxide nanoparticles using *Aspergillus fumigatus* JCF and characterization of synthesized nanoparticles. The anti-bacterial activity of biosynthesized zinc oxide nanoparticles was studied towards *K. pneumoniae*, *P. aeruginosa*, *E. coli*, *S. aureus* and *B. subtilis*.

In the preceding decade, nanotechnology has emerged as a technology that has altered every field of applied science. Nanoparticles are tiny particles ranging from 1 to 100 nm. NPs have unusual features because of their large surface-to-volume ratio and extremely small size, resulting in considerable variances in attributes compared to their bulk counterparts (Piccinno *et al.* 2012) [8]. By providing creative

solutions, nanoparticles have been successfully integrated into various sectors. ZnO is a type of metal nanoparticle made from metal oxides (Hedayati *et al.* 2017)^[9]. ZnO is an inorganic substance with distinctive features such as broad radiation absorption, pyroelectricity, semiconductor, high catalytic activity, and piezoelectricity (Sharma *et al.* 2011)^[10].

The current study focused on the biosynthesis of zinc oxide nanoparticles using SG1 (*Staphylococcus saprophyticus*), SG2 (*Brucella anthropi*), SG19 (*Citrobacter braaki*) and the subsequent characterization of the synthesized nanoparticles.

Materials and Methods

Materials: *Staphylococcus saprophyticus* (SG1), *Brucella anthropi* (SG2) and *Citrobacter braaki* (SG19) were

isolated from contaminated soil samples from industrial effluents. All these strains were grown on Luria-Bertani (LB) medium (Jayaseelan *et al.*, 2012)^[7].

Biosynthesis of ZnO nanoparticles: Bacterial cells were inoculated in conical flasks containing 50 mL of sterilized LB media and placed in a shaker incubator at 37° C and 120 rpm for 24 hrs. After the growth of bacteria, the media was inoculated with 0.1gm of ZnO by adjusting the pH to 6.5 and incubated in orbital shaker for 150 rpm at 32° C for 72 hrs. White precipitate deposition at the bottom of the flask indicated the formation of nanoparticles. White aggregate formed at the bottom of the flask was separated from the filtrate by centrifugation at 3000 rpm for 10 min and lyophilized (Baskar *et al.*, 2013)^[11].



Fig 1: precipitation of ZnO NPs at the bottom of the flasks

Characterization of ZnO NPs: For identification of zinc oxide nanoparticles, different analysis was used to verify the synthesis of the nanoparticles. Fourier transform infrared spectroscopy (FTIR; TENSOR 27, Bruker, Germany) was performed to examine the chemical functional groups of the samples. The synthesized nanoparticles were also analyzed by Energy Dispersive X-ray Spectroscopy (EDX) to identify the elements present in the sample by measuring the energy and intensity of X-rays emitted when the sample is exposed to an electron beam and Scanning Electron Microscopy (SEM) for investigating morphology and elemental compositions of the ZnO nanoparticles. The structural phase composition of the powder samples was characterized by X-ray diffraction (XRD; D8 Advance, Bruker, Germany) using Cu K α radiation at 35 kV and 30 mA. The XRD patterns were characterized by XRD evaluation software (DiffracPlus V1.01, Bruker, Germany).

Results

The process of synthesizing zinc oxide nanoparticles (ZnO NPs) involved three bacterial strains. During incubation period, precipitates began to develop and settled at the bottom of the flask, indicating the onset of transformation. These white sediments were not seen in the bacterial culture medium without the addition of ZnO NPs. The synthesized particles were characterized as described in the following sections

FT-IR spectrum analysis of Zinc Oxide Nanoparticles

The synthesized powders generated using three bacterial strains underwent FTIR analysis to identify the functional groups involved in biosynthesis. As shown in figure 2, FTIR spectra for SG1 showed a prominent peak at 3275 cm⁻¹ leads to water molecule –O-H stretching frequency. Further it showed a peak at 2971 cm⁻¹ responsible for aromatic ring. In addition, it exhibited at 1651 cm⁻¹ for C=O. Finally, it showed asymmetric stretching frequency at 1633 cm⁻¹, 1538 cm⁻¹, 1548 cm⁻¹ attributed for C=C and C-C bonds. On other hand SG2 showed a symmetrical stretching mode of vibration at 3359 cm⁻¹ and 3274 cm⁻¹ responsible for –O-H group (Miri *et al.*, 2019)^[13]. Aromatic carbon shown at 2924 cm⁻¹. Furthermore, prominent sharp peak at 1632 cm⁻¹ corresponding to C=O bond (Mahdi *et al.*, 2021)^[11]. Similarly, asymmetric stretching of –C-C=C- and -C=C observed at 1547 cm⁻¹, 1453 cm⁻¹ and 1401 cm⁻¹ respectively where as SG19 showed a broad peak at 3269 cm⁻¹ due to –O-H stretch of H₂O molecule. The peak at 2957 cm⁻¹ attributed to aromatic carbon. consequently at 1633 cm⁻¹ responsible for C=O carbonyl group, also peaks at 1565 cm⁻¹, 1537 cm⁻¹ and 1469 cm⁻¹ due to asymmetric stretching frequency of C-C and C=C bonds respectively.

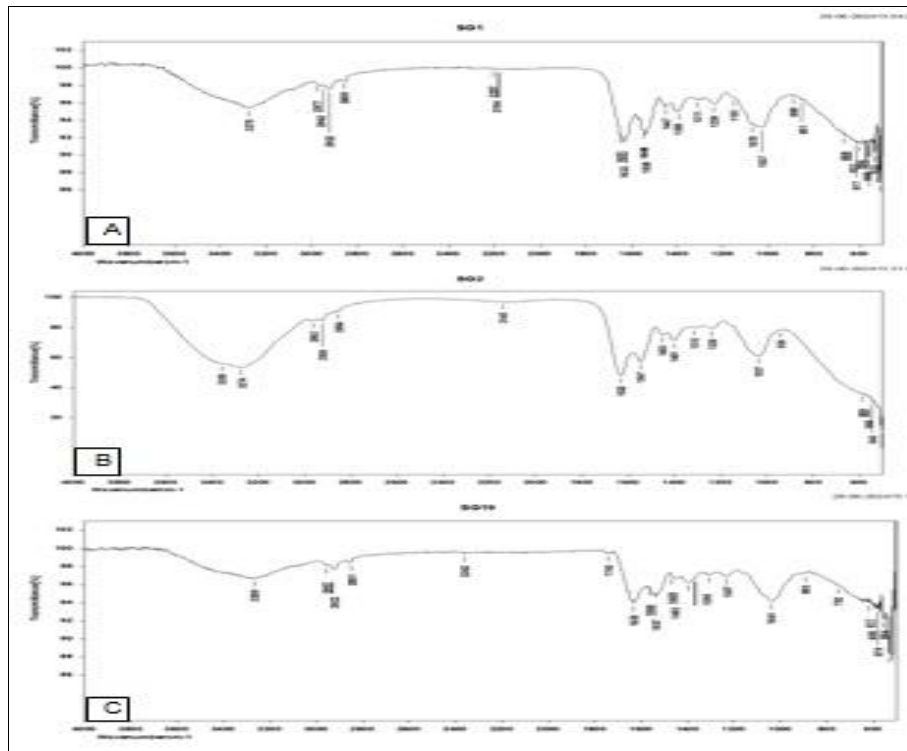


Fig 2: FTIR-spectrum of ZnONPs synthesized using (a) *S. saprophyticus* (b) *B. anthropi* (c) *C. braaki*

X-ray diffraction analysis

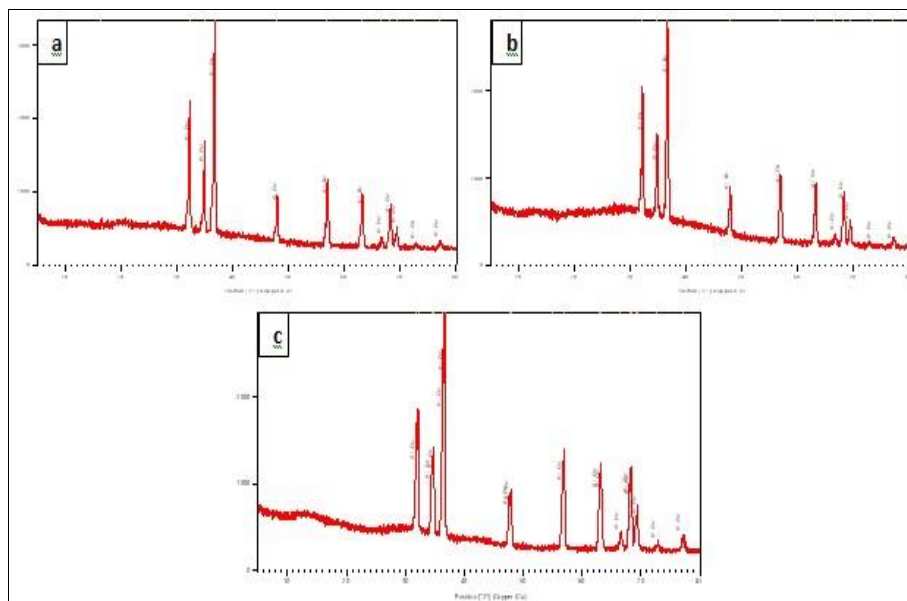


Fig 3: XRD analysis of synthesized ZnO NPs by (a) *S. saprophyticus* (b) *B. anthropi* (c) *C. braaki*

The phase purity and the crystallinity of the sample were examined by XRD diffraction technique. Figure 3 shows the XRD analysis of the ZnO particles synthesized by three heavy metal resistant bacteria. The XRD graph has shown 12 sharp diffraction peaks for *S. saprophyticus* in the 2θ range from 20° to 80° and the highest peak observed at position 36.6932 , height 2059.94 cts with relative intensity of 100% and the lowest peak was observed at position 16.3954 , height 5.48 cts with 0.27% relative intensity. As per the standard reference code 98-015-4487, the compound zincite shown the score of 50 with scale factor 0.320. The atomic arrangement or the compound were analyzed by d-

spacing [\AA], were maximum observed at 5.40223 \AA at peak position 16.394 2θ angle of height 5.48 cts and observed relative intensity of 0.27% with 0.0940 FWHM [$^\circ 2\theta$]. Minimum d-spacing was observed at 1.23610 \AA of peak position 77.0955 2θ angle of height 56.54 cts with relative intensity of 2.74% and 0.9576 FWHM [$^\circ 2\theta$]. By observing sharp peak on XRD graph, the compound zincite is crystalline in structure. In *B. anthropi*, the XRD graph showed 11 peaks and highest peak was observed at position 36.6043 2θ angle on X-axis with a peak height of 1659.59 cts with 100% relative intensity on Y-axis and the lowest peak was observed at position 73.3578 2θ angle on

X-axis of height 19.44cts with 1.17% relative intensity on Y-axis. As per the standard reference code 98-015-4487, the compound is zincite with having score of 68 with 0.531 scale factor. The atomic arrangement on the compound were analyzed by d- spacing [Å], were maximum observed at 2.78498 Å of peak position 32.1136 2θ angle of height 37.46cts with 3.3630 FWHM [°2θ]. By observing the sharp peak on the XRD graph the compound zincite with chemical formula ZnO is crystalline structure in nature. XRD graph has shown 19 peaks for *C. braaki* and highest peak were observed at position 36.3495 2θ angle of height 1852.6cts with 100% relative intensity and the lowest peak was

observed at position 55.0062 2θ angle of height 15.89cts with 0.86% relative intensity. As per the standard reference code 98-6-5119, the compound is zincite showing the score of 80 with 0.766 scale factor. The atomic arrangement on the compound analyzed by d- spacing [Å], were maximum observed at 2.80345 Å at peak position of 31.8964 2θ angle of height 776.33cts with 41% relative intensity showing at 0.4863 FWHM [°2θ]. By observing the peaks on the graph, the compound zincite may be semi crystalline in structure.

Energy Dispersive X-ray spectroscopy (EDX) and Scanning Electron Microscopy (SEM) analysis

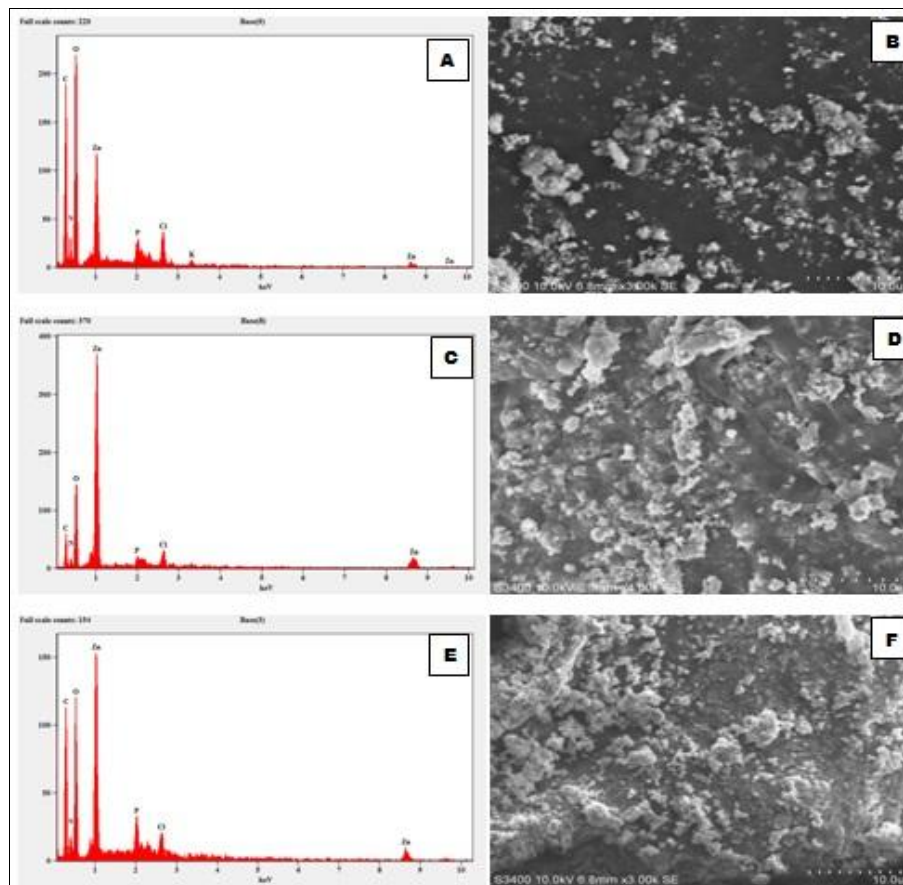


Fig 4: EDX and SEM micrographic image of synthesized ZnO NPs by (a) *S. saprophyticus* (b) *B. anthropi* (c) *C. braaki*

The analysis using Energy Dispersive X-ray Spectroscopy (EDX) provides insights into the chemical composition of the synthesized ZnO nanoparticles. Figure 4 displays the EDX spectrum, which was acquired in spot-profile mode from an area with a high concentration of ZnO nanoparticles. Notable signals corresponding to Zn atoms within the nanoparticles were detected, in addition to signals from C, O, P, and Cl atoms.

The SEM images of ZnO nanoparticles synthesized using *Staphylococcus saprophyticus*, *Brucella anthropi*, and *Citrobacter braaki* are displayed in Fig 4. Each of the three isolates demonstrates a variation in texture and differences in overall appearance. The SEM image of *S. saprophyticus* has a magnification power of X6.00K, revealing rod-shaped filamentous particles with an average diameter ranging from 230nm to 300nm. Active sites were identified on the surface of the adsorbent, leading to a transition from more heterogeneous to less heterogeneous surfaces. The most common organic texture found in this sample of in-situ bacteria is a buildup of a mucilaginous layer. The SEM

image for *B. anthropi* has a magnification power of X8.00K, showing that the sample with cultured bacteria has a globular microstructure, with average particle sizes between 200nm and 400nm. Active sites can be seen on the surface of the adsorbent. The main organic structure is affected by in-situ bacteria, resulting in a layer that does not accumulate. *C. braaki* appeared globular under a magnification of X6.00K, with average particle sizes of 300nm and 600nm, respectively. The primary organic structure consists of a thick layer of mucilaginous material.

Discussion

Biological synthesis of nanoparticles is an environmentally friendly, cost effective and non-toxic method (Li 2011). This study focuses on the development of ZnO NPs using *Staphylococcus saprophyticus*, *Brucella anthropi*, *Citrobacter braaki*. The findings revealed that *S. saprophyticus*, *B. anthropi*, *C. braaki* effectively synthesized ZnO NPs, and after 72 hours of interaction with zinc oxide powder, a white precipitate formed due to the

surface Plasmon resonance phenomenon. This aligns with Husssein et al. (2009), who highlighted *B. cereus* as a bio-template for producing zinc oxide nanoparticles. Additionally, Shamuzzan et al. (2014) proposed a simple and economical approach for synthesizing ZnONPs using *B. subtilis*. Also, Hsueh et al. (2015), reported the synthesis of ZnONPs using *B. cereus*. In addition, a biological approach for synthesizing ZnO NPs was outlined using innovative methodologies by Ghwas (2021). Salman et al. (2018) highlighted the synthesis of ZnO NPs using various *Lactobacillus* sp. Additionally, some researchers have explored the mechanisms underlying Zn nanoparticle synthesis by bacteria.

The FTIR data analysis was employed to determine the potential biomolecules responsible for the stabilization and capping of zinc oxide nanoparticles produced by *S. saprophyticus*, *B. anthropi*, *C. braaki*. The absorption band of ZnO particles synthesized by *S. saprophyticus*, *B. anthropi*, *C. braaki* exhibits greater prominence, increased intensity and broader characteristics compared to those of the other sample. These variations in wavenumber, peak shape and intensity suggests changes in the morphology and size of the ZnO particles (Abdullah et al., 2020). The presence of the amino and carbonyl functional groups observed in the FTIR spectra of the synthesized ZnO likely corresponds to cell membrane protein residues (Vimala et al., 2014). These proteins showed a strong capacity to bind metals, facilitating the capping of ZnO NPs (Ghwas 2021). This suggests that biological molecules can perform dual roles in both the formation and removal of metal nanoparticles (Vijayalakshmi et al. 2016).

The analysis of the XRD pattern for the synthesized ZnO NPs in the 2 θ range, along with its comparison to standard Bragg's diffraction peaks confirmed the characteristic crystalline structure (Shoeb et al., 2013) [14]. This was verified using the JCPDS card (no. 36-1451).

Bustos et al., 2018 [15] noted that biosynthesized nanoparticles on living cells were not only found on the cell surface but were also observed in the surrounding environment. It was suggested that nanoparticle biosynthesis might not solely involve adsorption. Instead it may also include bioaccumulation of metallic ions, followed by nanoparticle formation within the cells (Yusof et al., 2020). However, according to Zonaro et al., 2017 [17] extracellular ZnO nanoparticles were detected on cell surfaces, indicating that biosynthesis occurs through extracellular biotransformation facilitated by the cell membrane. The biosynthesized ZnO NPs were observed in SEM and the results indicated that *S. saprophyticus* appeared rod shaped filamentous whereas *B. anthropi* and *C. braaki* appeared as globular microstructure. While in another study ZnO NPs were reported to be like nanowires, spheroidal, geometrical shaped, irregular shaped and nano-rods (Hassan et al., 2020; Lopez-Cuenca et al., 2019; Umamaheswari et al., 2018).

Conclusions

The study demonstrated the synthesis of ZnO nanoparticles using *S. saprophyticus*, *B. anthropi*, *C. braaki*. The white precipitates of ZnO NPs were derived from a novel bacterial strain of *S. saprophyticus*, *B. anthropi*, *C. braaki* which were isolated from stressed soil samples (industrial sewage) from different regions of Karnataka, India. Heavy metal sorption was analyzed by X-ray diffraction. Zinc oxide nanoparticles of spherical structure were analyzed using

SEM and the functional groups present in the zinc oxide nanoparticles was confirmed by FT-IR analysis.

References

1. Mahdi ZS, Talebnia Roshan F, Nikzad M, Ezoji H. Biosynthesis of zinc oxide nanoparticles using bacteria: a study on the characterization application for electrochemical determination of bisphenol A. *Inorganic Nano-Metal Chemistry*, 2021;51(9):1249-1257.
2. Chen WH, Cheng HC, Hsu YC. Mechanical properties of carbon nanotubes using molecular dynamics simulations with the inlayer van der Waals interactions. *Computer Modeling in Engineering Sciences*, 2007;20(2):123.
3. Zhang X, Yan S, Tyagi RD, Surampalli RY. Synthesis of nanoparticles by microorganisms their application in enhancing microbiological reaction rates. *Chemosphere*, 2011;82(4):489-494.
4. Wang J, Chen C. Biosorbents for heavy metals removal their future. *Biotechnology advances*, 2009;27(2):195-226.
5. Hanley C, Layne J, Punnoose A, Reddy K, Coombs I, Coombs A, et al. Preferential killing of cancer cells activated human T cells using ZnO nanoparticles. *Nanotechnology*, 2008;19(29):295103.
6. Rajan A, Cherian E, Baskar G. Biosynthesis of zinc oxide nanoparticles using *Aspergillus fumigatus* JCF its antibacterial activity. *Int. J. Mod. Sci. Technol*, 2016;1(2):52-57.
7. Jayaseelan C, Rahuman AA, Kirthi AV, Marimuthu S, Santhoshkumar T, Bagavan A, et al. Novel microbial route to synthesize ZnO nanoparticles using *Aeromonas hydrophila* their activity against pathogenic bacteria fungi. *Spectrochimica Acta Part A: Molecular Biomolecular Spectroscopy*, 2012;90:78-84.
8. Piccinno F, Gottschalk F, Seeger S, Nowack B. Industrial production quantities uses of ten engineered nanomaterials in Europe the world. *Journal of nanoparticle research*, 2012;14:1-11.
9. Hedayati A, Darabitar F. Lethal sub-lethal impacts of lead on some hematological, biochemical immunological indices in Caspian roach (*Rutilus rutilus*). *Pollution*, 2017;3(1):21-27.
10. Sharma D, Sharma S, Kaith BS, Rajput J, Kaur M. Synthesis of ZnO nanoparticles using surfactant free in-air microwave method. *Applied Surface Science*, 2011;257(22):9661-9672.
11. Baskar G, Chandhuru J, Fahad KS, Praveen AS. Mycological synthesis, characterization antifungal activity of zinc oxide nanoparticles. *Asian Journal of Pharmacy Technology*, 2013;3(4):142-146.
12. Rahman Z, Thomas L, Singh VP. Biosorption of heavy metals by a lead (Pb) resistant bacterium, *Staphylococcus hominis* strain AMB-2. *Journal of basic microbiology*, 2019;59(5):477-486.
13. Miri A, Mahdinejad N, Ebrahimi O, Khatami M, Sarani M. Zinc Oxide Nanoparticles: Biosynthesis, Characterization, Antifungal Cytotoxic Activity. *Mater. Sci. Eng.: C*, 2019;104:109981 DOI: 10.1016/j.msec.2019.109981.
14. Shoeb M, Singh BR, Khan JA, Khan W, Singh BN, Singh HB et al. ROS-dependent anticandidal activity of zinc oxide nanoparticles synthesized by using egg albumen as a biotemplate. *Advances in Natural*

- Sciences:Nanoscience Nanotechnology,2013:4(3):0350-15.
15. Bustos MC, Ibarra H, Dussán J. The golden activity of *Lysinibacillus sphaericus*: new insights on gold accumulation possible nanoparticles biosynthesis. *Materials*, 2018. <https://doi.org/10.3390/ma11091587>.
 16. Mohd Yusof H, Abdul Rahman NA, Mohamad R, Zaidan UH, Samsudin AA. Biosynthesis of zinc oxide nanoparticles by cell-biomass supernatant of *Lactobacillus plantarum* TA4 its antibacterial biocompatibility properties. *Scientific reports*,2020:10(1):19996.
 17. Zonaro E, Piacenza E, Presentato A, Monti F, Dell'Anna R, Lampis S, *et al.* *Ochrobactrum* sp. MPV1 from a dump of roasted pyrites can be exploited as bacterial catalyst for the biogenesis of selenium tellurium nanoparticles. *Microbial cell factories*,2017:16:1-17.